Hindawi
Advances in Civil Engineering
Volume 2020, Article ID 8867678, 10 pages
https://doi.org/10.1155/2020/8867678

Research Article

Ultimate Pullout Capacity of a Square Plate Anchor in Clay with an Interbedded Stiff Layer

Tugen Feng, Jingyao Zong, Wei Jiang, Jian Zhang, and Jian Song

Key Laboratory of Ministry of Education for Geomechanics and Embankment Engineering, Hohai University, Nanjing, Jiangsu, China

Correspondence should be addressed to Jian Zhang; zhangj0507@hhu.edu.cn

Received 22 June 2020; Revised 4 August 2020; Accepted 29 August 2020; Published 10 September 2020

Academic Editor: Qiang Tang

Three-dimensional nonlinear numerical analysis is carried out to determine the ultimate pullout capacity of a square plate anchor in layered clay using the large finite element analysis software ABAQUS. An empirical formula for the pullout bearing capacity coefficient of a plate anchor in layered soils is proposed based on the bearing characteristics of plate anchors in single-layer soils. The results show that a circular flow (circulation field) is induced around the plate anchor during the uplift process and that the flow velocity and circulation field range are mainly affected by the properties of the soil around the plate anchor. The bearing characteristics of plate anchors in layered soils are influenced by factors such as the embedment depth of the plate anchor, the friction coefficient between the soil and the plate anchor, the thickness of the upper soil layer, and the thickness of the middle soil layer. The rationality of the finite element numerical calculation results and the empirical formula is verified by comparing the results from this study with results previously reported in the literature.

1. Introduction

Tension leg platforms, spar platforms, semisubmersible platforms, and other large floating structures are widely used in the exploration of underground resources in the deep sea. In contrast to offshore jacket platforms or gravity platforms, certain floating structures are supported by an anchor foundation (sustaining tension) that must be set in the seabed. One type of thin cylindrical shell structure is the suction embedded plate anchor foundation. Due to their advantages of accurate positioning, low cost, easy operation, and high vertical pullout bearing capacity, suction embedded plate anchor foundations have been used in deep-ocean exploitation (for example, as floating oil production platforms and other offshore platform foundations). Suction embedded plate anchor foundations are connected with the floating structure mainly through the mooring cable and bear the drawing load transmitted by the upper floating structure. Therefore, the uplift bearing characteristics of suction embedded plate anchors are the key characteristics that must be considered in the design and analysis of suction embedded plate anchor foundations.

The flow characteristics of the soil around plate anchors and the pullout bearing capacities of plate anchors have been studied by domestic and foreign scholars using numerical simulation methods, model tests, and the upper- and lower-bound limit analysis method [1, 2]. Wang et al. [3, 4] investigated the influences of the plate anchor shapes and the separation mode of the interface on the uplift bearing characteristics of plate anchors using the three-dimensional large deformation RITSS technique. Liu et al. [5] used the CEL technique (a fluid-solid coupling algorithm) in ABAQUS to analyze the large deformation of soils, and the variation rules of the complete load-displacement curves of plate anchors with different embedment depths and sizes were discussed. Athani et al. [6] and Evans and Zhang [7] analyzed the behavior of plate anchors during pullout in a granular assembly using the discrete element method, and the microscale physical processes were elucidated. Through numerous model tests, Das [8], Singh and Ramaswamy [9, 10], Liu et al. [11], Chow et al. [12], and Dash and Choudhary [13] determined the pullout bearing capacities of plate anchors of different sizes and at different depths in soft

clay and sandy soil. Using centrifugal model tests, Gaudin et al. [14], Gaudin et al. [15], Randolph et al. [16], and Song et al. [17] studied the "keying" process in the installation of suction embedded plate anchors. The results show that the "keying" process can reduce the embedment depth of the anchor body, which reduces the pullout bearing capacity of the plate anchor. Through centrifuge model tests, Blake [18] analyzed the effects of soil consolidation on the pullout bearing capacity of plate anchors after their installation. Based on generalized plastic limit analysis, Yang et al. [19] and Lu [20] put forward analysis models of the "keying" process of suction embedded plate anchors and predicted the movement path and pullout bearing capacity of suction embedded plate anchors under different loading conditions. Merifield et al. [21] and Merifield et al. [22] studied the bearing behavior of horizontal and vertical plate anchors in homogeneous and heterogeneous soils using the upper- and lower-bound finite element method and discussed the effects of the embedment depth, roughness coefficient, overburden pressure, and plate anchor material properties on the pullout bearing capacity.

Although the bearing characteristics of plate anchors have been reported, most existing reports have mainly focused on cases in single-layer soil. In practical engineering, layered soils are also common. The bearing characteristics of plate anchors in layered soils are obviously different from those in single-layer soil. At present, little research has been performed on the bearing mechanisms of plate anchors in layered soils, especially for cases with large differences between the properties of the lower and upper soil layers. Therefore, considering stratum heterogeneity, a finite element analysis model of the pullout bearing capacity of square plate anchors in layered clay is established using the CEL technique and the finite element analysis software ABAQUS. The differences in the (i) circulation field and (ii) pullout bearing characteristics of the plate anchors between the single-layer and layered soils are discussed, and an empirical formula for the pullout bearing capacity of plate anchors in layered soils is proposed.

2. Finite Element Calculation Model

Das [23] and Das et al. [24] noted that the pullout bearing capacity Q_u of a plate anchor during normal operation (in general working conditions) includes the net pullout bearing capacity Q_n, the suction force F_s, and the anchor weight W_a. The suction force is generated due to the difference in the superstatic pore water pressure on the upper and lower surfaces of the plate anchor. Suction is often neglected in engineering design, and the resulting conservative design is beneficial for engineering safety. The influence of suction force is not considered in the calculations detailed in this paper.

3. Establishment of a Linear Programming Model

A model of the pullout bearing capacity of a square plate anchor is established using ABAQUS finite-element analysis software. As shown in Figure 1, a 1/4 calculation model is established considering the symmetry of the plate anchor. The length L and width B of the plate anchor are $L = B = 2$ m, and the thickness is $t = 0.3$ m. The length and width of the model are taken as $10B$. As shown in Figure 2, the soil in the model is divided into three layers (layered soils): the upper soil, middle soil, and lower soil. The interface between the upper soil and middle soil is defined as interface 1, and the interface between the middle soil and the lower soil is defined as interface 2. The horizontal and vertical displacement components are set to zero at the bottom of the model, and the horizontal displacement component is equal to zero around the model. The plate anchor is set as a rigid body by applying rigid constraints, and rigid C3D8R elements are used to simulate the plate anchor. EC3D8R elements are applied to simulate the soil. The roughness coefficient between the plate anchor and the soil is assumed to be 0.3 [15]. The mesh size is adjusted according to the calculation accuracy and the calculation time limit, and a mesh pattern is presented to ensure that the mesh density gradually increases toward the periphery of the plate anchor. The soil mass surrounding the plate anchor is established as a Tresca material [4]. The soil property parameters are selected and simplified according to the results of a field test of marine soft soil performed by Stewart and Randolph [25], Ou et al. [26], and Zhang et al. [27]. The layered soil parameters are shown in Figure 2. For normally consolidated soil (upper and lower soil layers), the undrained shear strength is set to $s_u = s_{u,\min} + kH$. The initial value is $s_{u,\min} = 0.5$ kPa, and the slope is $k = 1$ kPa/m. The middle soil is assumed to be homogeneous, and its undrained shear strength is set to $s_{u2} = 40$ kPa. The undrained shear strengths of the soils at interface 1 and interface 2 are set according to the shear strength of normally consolidated soil. The soil weight of these three soil layers is 16.5 kN/m^3, and the elastic modulus E is $500s_u$ [28–30]. The lateral Earth pressure coefficient K_0 of the soil is 1.0, and Poisson's ratio μ is set to 0.49.

The pullout bearing capacity of a square plate anchor is obtained through two steps. In the first step, the initial ground stress balance of the model is calculated, and the original consolidation state of the marine soil is simulated. In the second step, uniform upward displacement is applied to the plate anchor so that the plate anchor is pulled upward uniformly, and the variations in the pullout bearing capacity of the plate anchor with uplift displacement are obtained. The stabilized load is selected as the ultimate pullout bearing capacity of the plate anchor.

4. Comparison of the Pullout Bearing Capacity Coefficients Determined by the Proposed Method and Those Presented in the Literature for a Plate Anchor in Single -Layer Soil

The pullout bearing capacity-displacement curve of the plate anchor indicates that the pullout bearing capacity of the plate anchor increases and then stabilizes when the displacement increases. When the fluctuation range of the

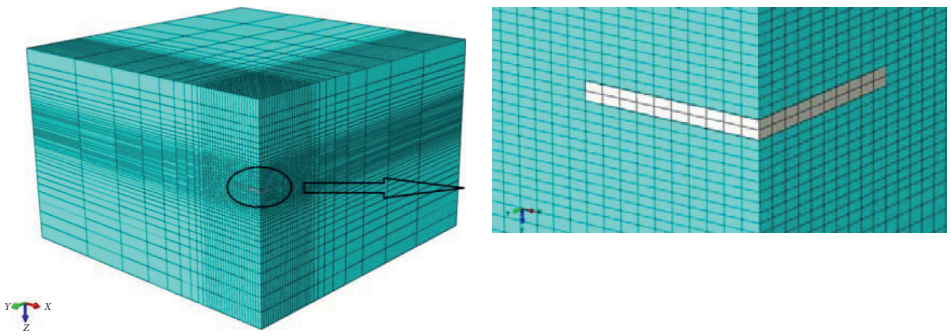

(a) (b)

Figure 1: Mesh layout of the analysis model.

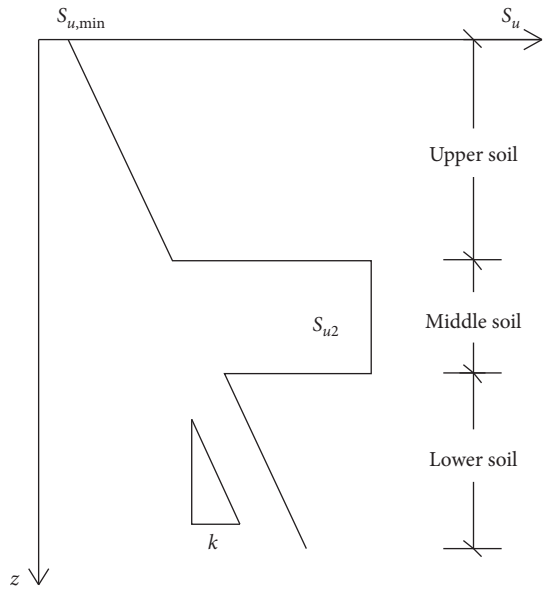

Figure 2: Layered soil parameters.

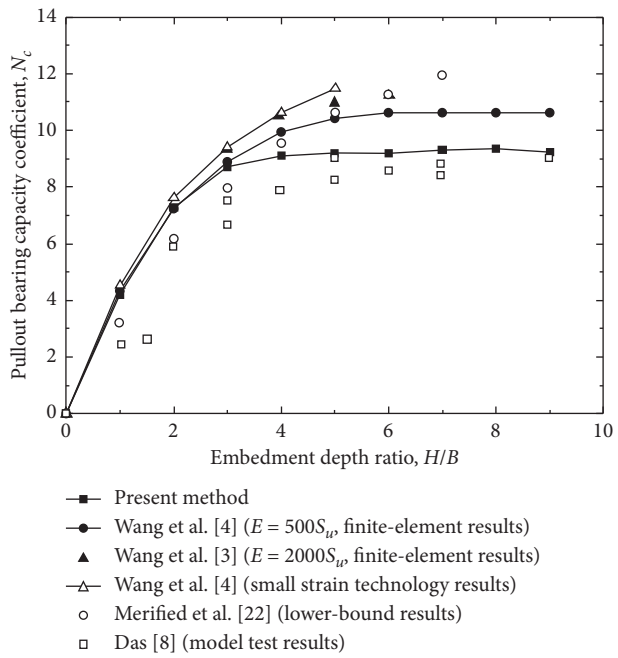

Figure 3: Variation in the pullout bearing capacity coefficient of the plate anchor with the H/B.

pullout bearing capacity of the plate anchor does not exceed 10% [5], it is assumed that the steady state has been reached and that the average value of the pullout bearing capacity in this steady state is the net ultimate pullout bearing capacity Q_n of the plate anchor. The pullout bearing capacity coefficient N_c of the plate anchor can be obtained by formula (1) [5].

$$N_c = \frac{Q_n - \gamma AH}{As_u}, \tag{1}$$

where A is the area of the plate anchor and H is the embedment depth of the plate anchor.

Figure 3 shows the computed N_c in the single-layer soil when the undrained shear strength is $s_u = s_{u,\min} + kH$, the initial value is $s_{u,\min} = 0.5$ kPa, and the slope is $k = 1$ kPa/m. To verify the rationality of the above analysis model, Figure 3 also shows the N_c results obtained using the finite element method [3, 4], the lower-bound finite element method [22], and the model test method [8]. Figure 3 shows that although the analysis methods are different, the variation rules of N_c are similar. N_c increases as the embedment depth H/B increases. When H/B reaches a certain depth, N_c tends to be stable. In addition, Figure 3 shows that the calculation results agree well with the results of Wang et al. [3, 4] before N_c is stable. For a stable N_c, the results calculated in this paper are smaller than those of Wang et al. [3, 4] but are similar to the results of the model test method [8]. The above analysis shows that it is feasible to analyze the bearing characteristics of the plate anchor by using the three-dimensional nonlinear numerical analysis presented in this paper.

5. Soil Flow Characteristics during the Uplift of the Plate Anchor

In the process of pulling up the plate anchor, the flow characteristics of the soils around the plate anchor can influence the ultimate pullout capacity of the plate anchor. Thus, in this section, the differences in the flow laws between the layered soils and the single-layer soil are discussed.

Because of the large difference in the properties between the middle soil layer and the upper and lower soil layers, the flow law of the layered soils around the plate anchor is different from that of the single-layer soil, which results in a difference in the pullout bearing characteristic of the plate anchor. It is assumed that the thickness of the upper soil layer is $H_1 = 6$ m and that the thickness of the middle soil layer is $H_2 = 6$ m. Figure 4 shows the flow of the soil around the plate anchor. The plate anchor is buried at interface 1 ($H = 6$ m), and the vertical displacement for the plate anchor is $0.04B$ (when the displacement of the plate anchor in the vertical direction exceeds $0.02B$, the flow law of the surrounding soil remains stable). As shown in Figure 4(a), a complete circulation field can form around the plate anchor in single-layer soil. In the layered soils, the upper part of the soil exhibits a circulation trend. However, the soil cannot flow freely when it refluxes to interface 1 because of the differences in the properties of the upper and middle soil layers. In addition, Figure 4 shows that, for layered soils, the flow velocities of the soils around the plate anchor are smaller than those in the single-layer soil because of the existence of the middle soil layer.

The flow of the surrounding soil when the plate anchor was buried in the middle soil layer ($H = 10$ m) is shown in Figure 5. A complete circulation field can be formed in both the layered soils and single-layer soil. For the layered soils, the bottom of the circulation field extends to only interface 2 and cannot affect the lower soil. However, because the plate anchor is restricted by the hard soil around it, the horizontal displacement of the soil above the plate anchor in the layered soils case is larger than that in the single-layer soil case.

The soil flow when the plate anchor is located at interface 2 ($H = 12$ m) is shown in Figure 6. A complete circulation field can be formed in both the layered soils and single-layer soil. At this time, the horizontal displacement of the soil above the plate anchor in the layered soils is larger than that in the single-layer soil. The soil at the bottom of the plate anchor mainly deforms vertically upward.

6. Variations in the Pullout Bearing Capacity Coefficient

From the above analysis, the soil flow deformation around the plate anchor in the layered soils is different from that in the single-layer soil. Therefore, the bearing characteristics under the two conditions are different. The pullout bearing characteristic of the plate anchor is mainly influenced by the embedment depth, the soil properties, the friction coefficient between the soil and the plate anchor, the lateral pressure coefficient, the soil layer thicknesses, and the plate anchor shape. Because studies of the influences of the plate anchor size and shape on the pullout bearing capacity have been performed, the influences of other factors on the variation laws of the pullout bearing capacity are discussed in this paper. Trial calculation suggests that the lateral pressure coefficient has little effect on the pullout bearing capacity coefficient. When the lateral pressure coefficient varies within 0~1.0, the pullout bearing capacity coefficient changes within 3.5%. To facilitate analytical analysis, the lateral pressure coefficient is assumed to be 1.0 in this paper.

6.1. Embedment Depth. Figure 7 shows the pullout bearing capacity coefficient of the plate anchor $N_{c,l}$ at different embedment depths H/B ($H_1 = 3B$, $H_2 = 3B$, $\alpha = 0.3$) in the layered soils. H/B ranges from 1 to 9. For comparative analysis, the N_c calculated in the single-layer soil is also plotted in Figure 7.

Figure 7 shows that when $H/B < 2$, the $N_{c,l}$ values of the layered soils are slightly larger than those of the single-layer soil. When $H/B > 2$, the $N_{c,l}$ values of the layered soils are slightly lower than those in the single-layer soil. Combined with Figure 4, when the embedment depth of the plate anchor approaches interface 1, the area (resisting the soil flow deformation) at the bottom of the plate anchor in the layered soils is smaller than that in the single-layer soil, so its pullout bearing capacity decreases to some extent. When the plate anchor is located in the hard middle soil layer, the $N_{c,l}$ values of the layered soils are significantly larger than those in the single-layer soil because the ability of the middle hard soil to resist deformation is larger than that of a single layer of normally consolidated soil. As H/B increases, $N_{c,l}$ increases first and then decreases. When $H/B = 5$, $N_{c,l}$ reaches the maximum value. When the plate anchor is located at the lower soil layer, the $N_{c,l}$ values are slightly larger than those of the single-layer soil, but the difference decreases gradually with increasing H/B.

6.2. Upper Soil Thickness. As shown in Figure 8, different embedment depths of the plate anchor are selected to study the influence of the upper soil thickness H_1 on $N_{c,l}$: (i) near interface 1 (position A: $H = H_1 - 0.5B$ and position B: $H = H_1 + 0.5B$), (ii) near interface 2 (position C: $H = H_1 + H_2 - 0.5B$ and position D: $H = H_1 + H_2 + 0.5B$), and (iii) at a more central position (position E: $H = H_1 + 2B$). The value of α is 0.3 for this investigation.

Figure 9 shows the variation in $N_{c,l}$ with H_1 when the plate anchor is located at positions A through E. At position A, $N_{c,l}$ increases with increasing H_1. When the plate anchor is located at position B, $N_{c,l}$ increases with H_1 until H_1 reaches 4 m; then, $N_{c,l}$ remains basically unchanged with increasing H_1. At position C, $N_{c,l}$ remains stable as H_1 increases until H_1 reaches 4 m; then, $N_{c,l}$ decreases slightly. At position D, $N_{c,l}$ remains stable as H_1 increases. When the plate anchor is located at position E, $N_{c,l}$ decreases gradually as H_1 increases, and the rate of decrease slows when H_1 approaches 6 m.

6.3. Thickness of the Hard Middle Soil Layer. Because the change in thickness of the hard middle soil layer H_2 has little effect on the pullout bearing characteristic of the plate anchor buried at positions A and B, the influences at positions A and B are not discussed here. In addition, when the thickness of the hard middle soil layer changes, position E is located near position C, near position D, or in the lower soil. Thus, in this paper, the effect of H_2 on the pullout bearing characteristic of the plate anchor is studied at only positions C and D, and the pullout bearing characteristic of the plate anchor at position E is not discussed separately.

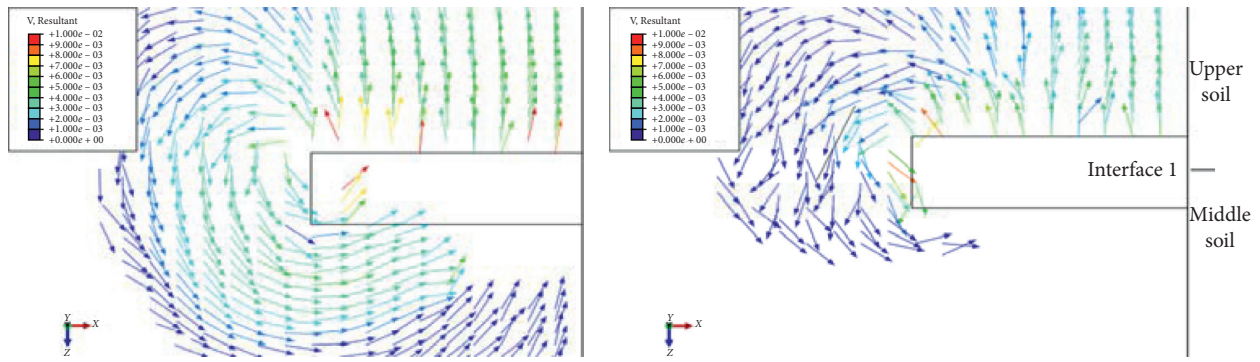

Figure 4: Soil flow under different formation conditions ($H = 6$ m). (a) Single-layer soil. (b) Layered soils.

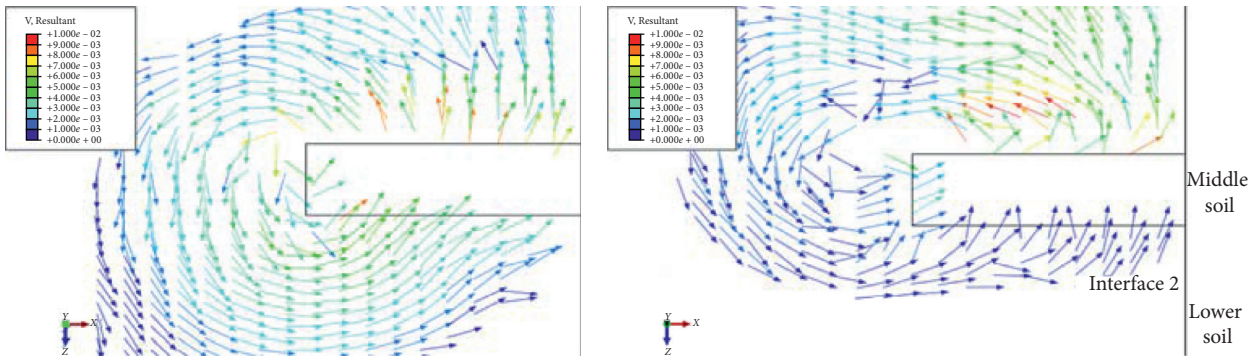

Figure 5: Soil flow under different formation conditions ($H = 10$ m). (a) Single-layer soil. (b) Layered soils.

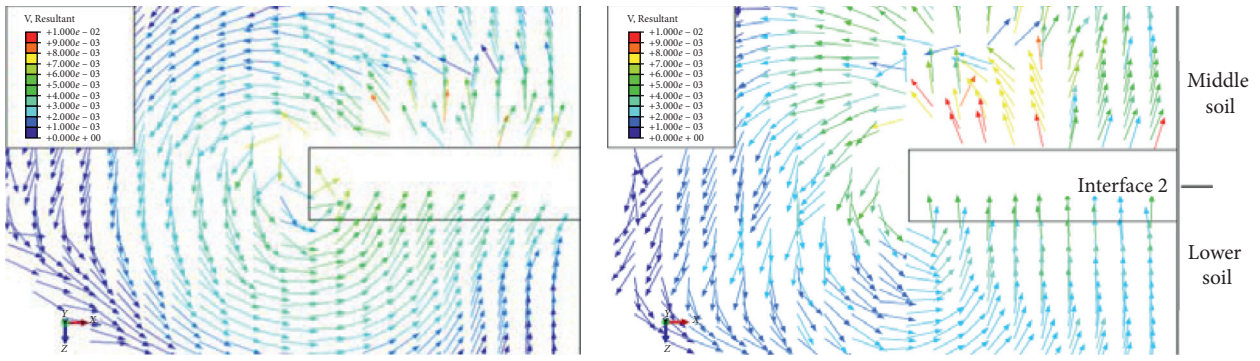

Figure 6: Soil flow under different formation conditions ($H = 12$ m). (a) Single-layer soil. (b) Layered soils.

Figure 10 shows the variation in $N_{c,l}$ with the thickness of the hard middle soil layer H_2 ($H_1 = 3B$, $\alpha = 0.3$). When the plate anchor is located at position C, $N_{c,l}$ first increases and then stabilizes with increasing H_2. When H_2 is large ($H_2/B \geq 2.5$), the change in H_2 has less effect on $N_{c,l}$. Compared with the results of the single-layer soil, $N_{c,l}$ at position C is affected by interface 2 in the layered soils. When the difference in strength between the hard middle soil and the lower soil layers around interface 2 is small, $N_{c,l}$ at position C in the layered soils is close to that of the single-layer soil. When the plate anchor is located at position D, $N_{c,l}$ decreases only slightly with increasing H_2.

7. Friction Coefficient between the Plate Anchor and Soil

To analyze the influence of the friction coefficient α between the plate anchor and soil on the bearing characteristic of the plate anchor, the following values of α were considered: 0, 0.3, 0.5, 0.7, and 1.0. Figure 11 shows the variation in $N_{c,l}$ with α

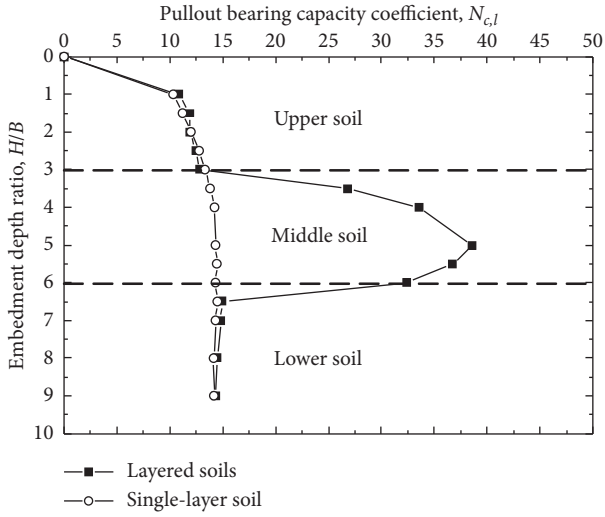

Figure 7: Variation in the pullout bearing capacity coefficient at different embedment depths ($H_1 = 3B$, $H_2 = 3B$, $\alpha = 0.3$).

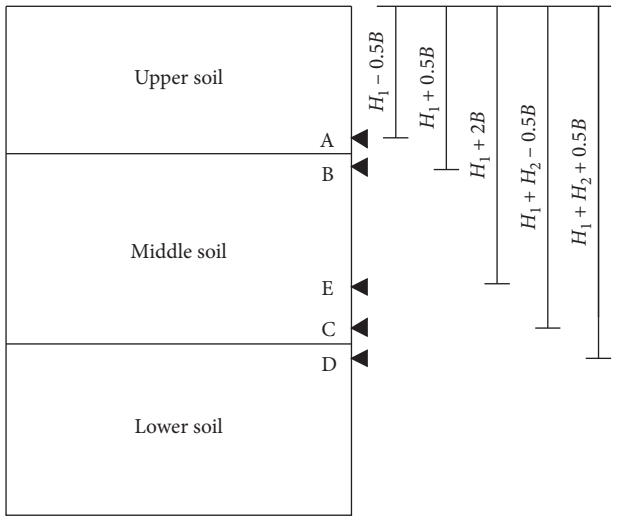

Figure 8: Diagram of the plate anchor buried at different positions.

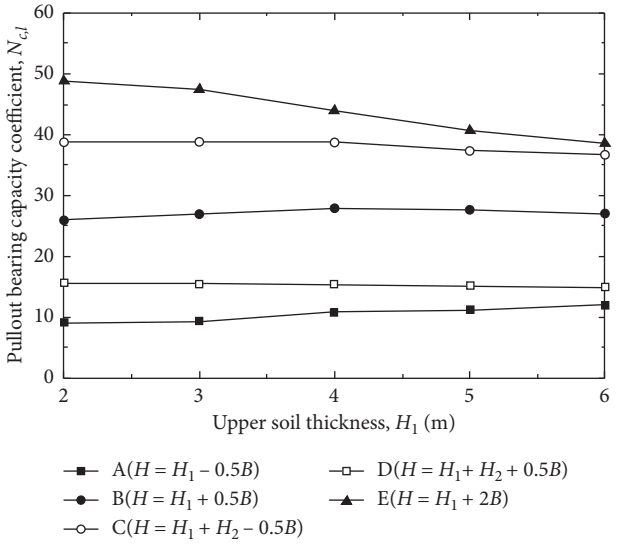

Figure 9: Variation in $N_{c,l}$ with the upper soil thickness H_1 ($\alpha = 0.3$).

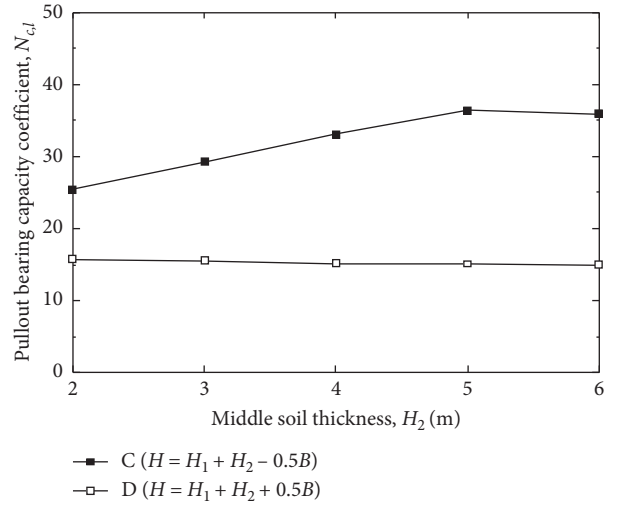

Figure 10: Variation in $N_{c,l}$ with the thickness of the hard middle soil layer H_2 ($H_1 = 3B$, $\alpha = 0.3$).

($H_1 = 3B$, $H_2 = 3B$). $N_{c,l}$ clearly increases with α, but the rate of increase gradually decreases. When α exceeds 1.0, the contribution of an increase in α to the increase in $N_{c,l}$ is small.

7.1. Plate Anchor Design in Layered Soils

7.1.1. Formula for Calculating the Pullout Bearing Capacity Coefficient of a Plate Anchor. By comparing the pullout bearing characteristics of the plate anchor in the single-layer soil, it was found that influence coefficients related to different factors can be proposed. The pullout bearing capacity coefficient of the plate anchor in layered soils can be obtained by combining the formula for calculating the pullout bearing capacity coefficient in the single-layer soil and the influence coefficients.

Figure 12 shows the variation in N_c in the single-layer soil. N_c increases with increasing H/B, and when $H/B \geq 5$, N_c remains stable. The pullout bearing capacity coefficients in the single-layer soil can be expressed as

$$N_c = \begin{cases} -0.2598\left(\dfrac{H}{B}\right)^2 + 2.586\left(\dfrac{H}{B}\right) + 7.565, & \dfrac{H}{B} < 5, \\ 14, & \dfrac{H}{B} \geq 5. \end{cases} \quad (2)$$

By comparing the pullout bearing capacity coefficient in the layered and single-layer soils, the relationships between the embedment depth H of the plate anchor, the thickness H_1 of the upper soil, the thickness H_2 of the hard middle soil layer, and the pullout bearing capacity coefficient in the layered soils $N_{c,l}$ were obtained.

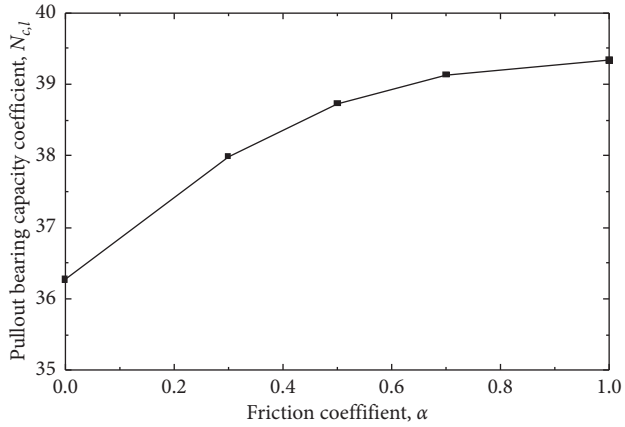

Figure 11: Variation in $N_{c,l}$ with the friction coefficient between the plate anchor and soil α ($H_1 = 6$ m, $H_2 = 6$ m).

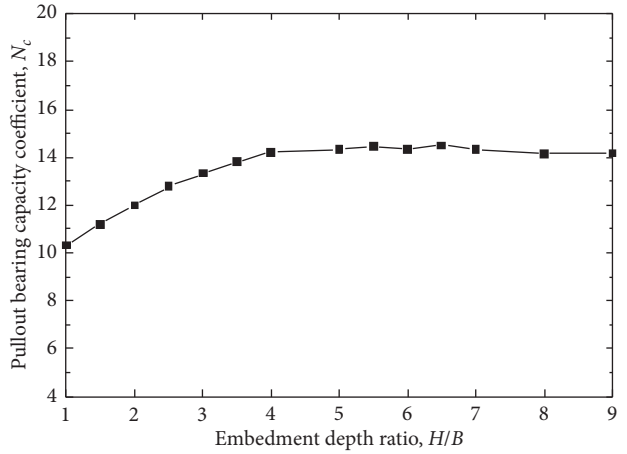

Figure 12: Variation in N_c with embedment depth in the single-layer soil (normally consolidated soil).

$$N_{c,l} = N_c \cdot \beta_H \cdot \beta_\alpha. \tag{3}$$

The influence coefficient β_H related to H, H_1, and H_2 can be expressed as

$$\beta_H = \begin{cases} 0.9, & H \le H_1, \\ \left[-0.5066\left(\dfrac{H}{B}\right) + 5.1737\right] \times \alpha_H, & H_1 \le H < H_1 + H_2, \\ 1.0, & H > H_1 + H_2, \end{cases} \tag{4}$$

where α_H is the interface influence coefficient, which is related to the position of the plate anchor in the hard middle soil layer. When the distance between interface 1 and the plate anchor is 1B, α_H is 0.5. When the distance between interface 1 and the plate anchor is greater than 2B and the distance between interface 2 and the plate anchor is greater than 1B, $N_{c,l}$ is not affected by the interface (α_H is 1.0). When the distance between interface 1 and the plate anchor is greater than 2B, and the distance between interface 2 and the plate anchor is 1B, $N_{c,l}$ is not affected by interface 1. α_H is influenced by the shear strength ratio at interface 2 and can be obtained through the following expression:

$$\alpha_H = -0.1285\left(\frac{s_{u2}}{s_{u3}}\right) + 1.4921, \tag{5}$$

where s_{u3} is the shear strength at interface 2.

The influence coefficient β_α related to α can be expressed as

$$\beta_\alpha = \begin{cases} -0.0971\alpha^2 + 0.1771\alpha + 0.9557, & H_1 < H \le H_1 + H_2, \\ 1.0, & H \le H_1 \text{ or } H > H_1 + H_2. \end{cases} \quad 0 \le \alpha \le 1.0, \tag{6}$$

8. Verification of the Pullout Bearing Capacity Formula

Two types of geotechnical conditions were selected to verify the rationality and applicability of formula (3), and the numerical results and empirical results are listed in Table 1.

Table 1 shows that when the plate anchor is located near interface 1, the numerical result of $N_{c,l}$ is 11.70, and the empirical calculation result is 11.37. The numerical result is slightly higher (2.90% higher) than the empirical calculation result. When the plate anchor is located near interface 2, the numerical result of $N_{c,l}$ is 40.26, and the calculated result is 39.40. The numerical result is slightly higher (2.18% higher) than the calculated result. This comparison shows that the empirical calculation results are slightly lower than the numerical results and that the differences are small. Thus, it is reasonable to use the above-mentioned formula to guide the design of the pullout bearing capacity of plate anchors in layered soils.

9. Discussion

In the installation process, the plate anchor first sinks to the design embedment depth and then is rotated to the design angle by tethers, resulting in a certain loss of embedment depth. The loss of embedment depth will lead to a decrease in the bearing capacity and the anchoring effect, so it is necessary to adjust the installation of the plate anchor, reducing or even eliminating the loss of embedment depth during the installation process to guarantee stable anchoring effect. As shown in Figure 13, in this section, an improved installation system of the plate anchor is discussed to avoid the loss of embedment depth. In this installation system, the rotation of the plate anchor is controlled by upper and lower gears

Table 1: Verification of the pullout bearing capacity formula.

	Working condition ($L = B = 2$ m)	Pullout bearing capacity coefficient $N_{c,l}$		Difference (%)
		Numerical result	Formula result	
1	$H_1 = 5$ m, $H_2 = 4$ m, $H = 4$ m, $\alpha = 0.2$	11.70	11.37	2.90
2	$H_1 = 5$ m, $H_2 = 5$ m, $H = 9$ m, $\alpha = 0.6$	40.26	39.40	2.18

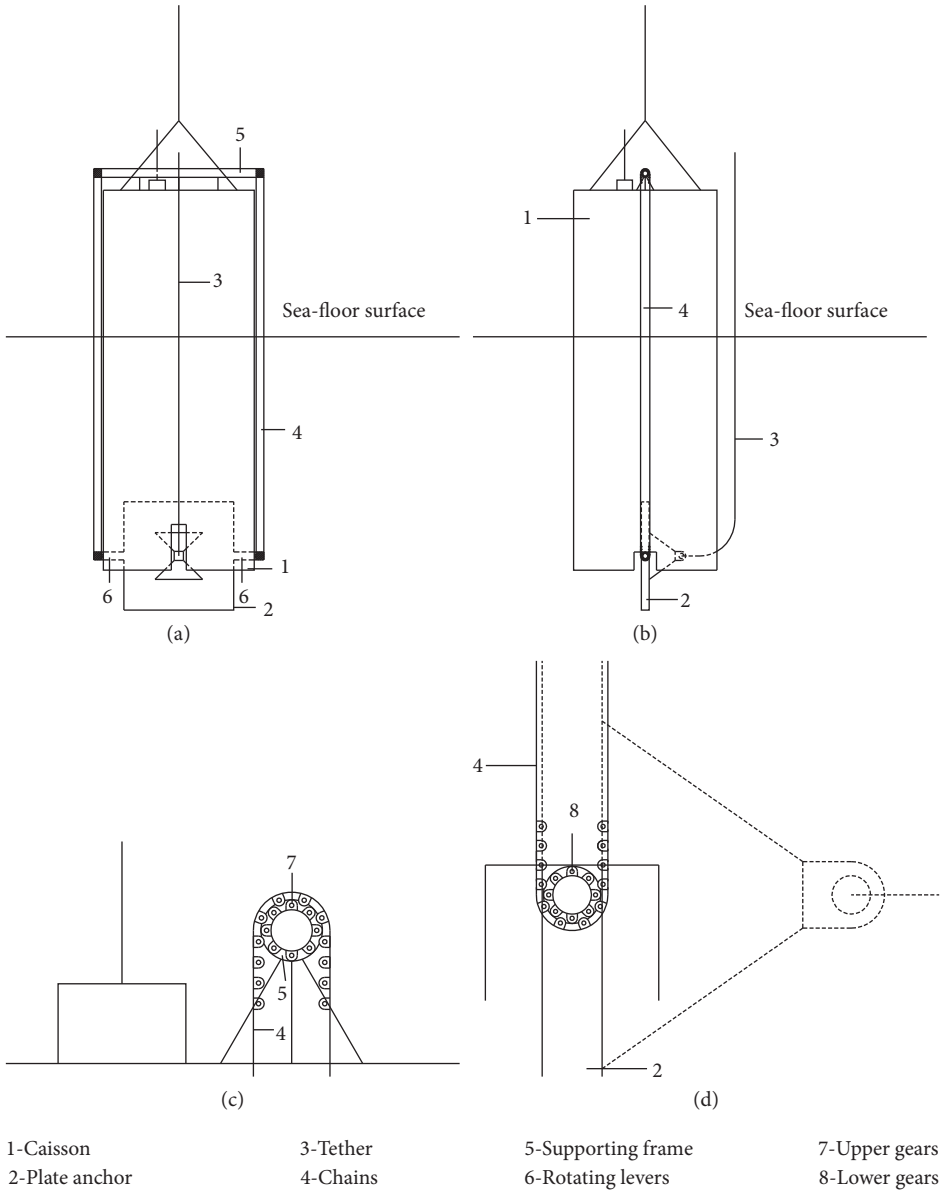

Figure 13: Improved installation system of the plate anchor. (a) Front view. (b) Side view. (c) Detailed view of the upper gears. (d) Detailed view of the lower gears.

through chains transmitting power. The height-adjustable supporting frame is equipped on the top of the caisson and the upper gears are set at the supporting frame. Both sides of the plate anchor are connected to the rotating levers, and the levers are fit into sockets set on the bottom of the caisson. The lower gears are fixed at the plate anchor and connected with the upper gears with chains. By transmitting power between the upper and lower gears through chains, the plate anchor is rotated to the design angle.

The improved installation process of the plate anchor is shown in Figure 14. During the overall installation process, the plate anchor first sinks with the caisson, and the chains between the upper and lower gears remain under tension in the sinking process. After the plate anchor sinks to the

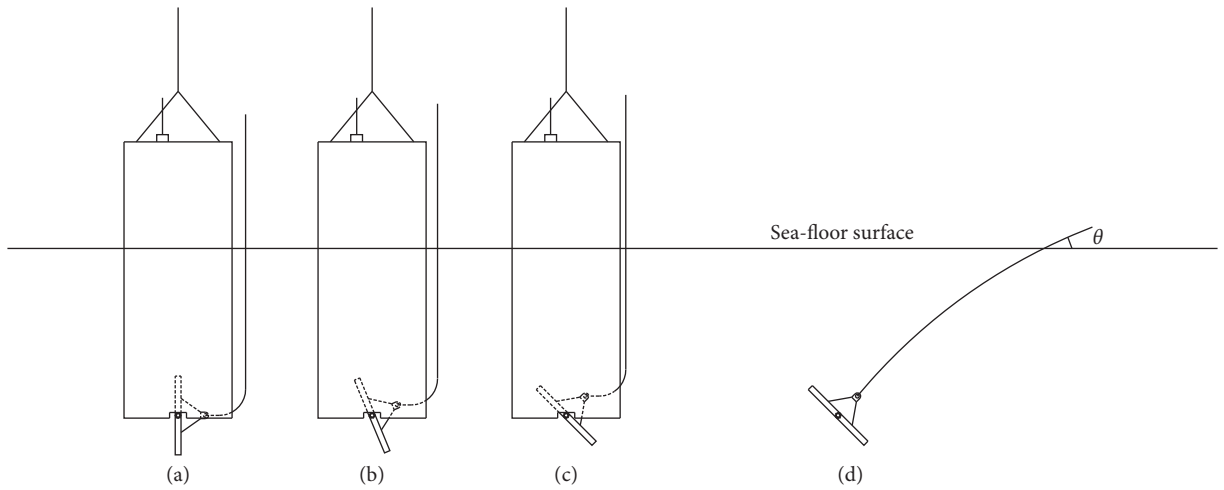

Figure 14: Improved installation process of the plate anchor.

design embedment depth, the upper gears are rotated to rotate the lower gears, and then the plate anchor is driven by the rotation of the lower gears to the design angle. The rotation of the upper gears is stopped when the plate anchor reaches the design angle, the chains between the upper and lower gears are loosened by lowering the support frames, and then the chains are separated from the lower gears. By pulling on the caisson, the upper gears and the chains break away from the plate anchor. Subsequently, by fixing tethers connected with the plate anchor to the floating platform, the installation of the plate anchor is completed. In addition, the support frame described in this installation system is used to support the upper gears on the top of the caisson. After the plate anchor is rotated to the design angle, the installation system can be evacuated, and the chains between the upper and lower gears are loosened by adjusting the height of the height-adjustable support frame. Then, other machinery is used to pull up the caisson, together with the upper gears and the chains, to complete the evacuation.

This improved installation system uses gears to rotate the plate anchor to the design angle without the loss of embedment depth. It is beneficial to ensure the bearing capacity of the plate anchor to a certain extent.

10. Conclusions

General finite element analysis software is applied to study the ultimate uplift bearing characteristics of a plate anchor in layered soils, and empirical formula for the pullout bearing capacity coefficient of a plate anchor in layered soils is proposed.

(1) The circular flowing trend of the soil surrounding a plate anchor in layered soils is similar to that in a single layer of soil during the process of plate anchor uplift. When the plate anchor is located near interface 1, the circular flow of the soil stagnates at the interface. When the plate anchor is buried near interface 2, a complete circulation field forms because the difference in the soil properties between the middle and lower soil layers is relatively small.

(2) The $N_{c,l}$ values in the layered soils increase with increasing α. When the plate anchor is located in the hard middle soil layer, $N_{c,l}$ is greater than those when the plate anchor is located in the other two soil layers, and $N_{c,l}$ first increases and then decreases with increasing embedment depth. When the plate anchor is buried near interface 1, $N_{c,l}$ increases to a certain extent as the upper soil thickness H_1 increases. As the thickness of the hard middle soil layer H_2 increases, the $N_{c,l}$ of the plate anchor located near the top of interface 2 increases, and the influence of H_2 on the $N_{c,l}$ of plate anchors buried at other positions is small.

(3) Based on the bearing characteristics of a plate anchor in single-layer soil, an empirical formula of the pullout bearing capacity coefficient for plate anchors in layered soils is proposed in terms of the embedment depth, upper soil thickness, hard middle soil thickness, and friction coefficient.

Data Availability

The data used to support the findings of this study are available from the corresponding author upon request.

Conflicts of Interest

There are no conflicts of interest regarding the publication of this paper.

Authors' Contributions

Tugen Feng and Jingyao Zong made contributions to the analysis and paper writing. Wei Jiang contributed to the calculations in this paper. Jian Zhang made contributions to the calculations, paper writing, and analysis. Jian Song gave some significant suggestions on the design of the plate anchor in the revised version, so he is added.

Acknowledgments

This work was sponsored by the Fundamental Research Funds for the Central Universities (nos. B200204032 and 2019B07914) and the National Natural Science Foundation of China (No. 51808193). The authors are grateful for this support.

References

[1] J. Zhang, J. Yang, F. Yang, X. Zhang, and X. Zheng, "Upper-bound solution for stability number of elliptical tunnel in cohesionless soils," *International Journal of Geomechanics*, vol. 17, no. 1, p. 06016011, 2017.

[2] J. Zhang, T. Feng, J. Yang, F. Yang, and Y. Gao, "Upper-bound stability analysis of dual unlined horseshoe-shaped tunnels subjected to gravity," *Computers and Geotechnics*, vol. 97, pp. 103–110, 2018.

[3] D. Wang, Y. X. Hu, and M. F. Randolph, "Effect of loading rate on the uplift capacity of plate anchors," in *Proceedings of the Eighteenth International Offshore and Polar Engineering Conference*, Vancouver, Canada, 2008.

[4] D. Wang, Y. Hu, and M. F. Randolph, "Three-dimensional large deformation finite-element analysis of plate anchors in uniform clay," *Journal of Geotechnical and Geoenvironmental Engineering*, vol. 136, no. 2, pp. 355–365, 2010.

[5] H. Liu, F. Su, and Z. Li, "The criterion for determining the ultimate pullout capacity of plate anchors in clay by numerical analysis," *American Journal of Engineering and Applied Sciences*, vol. 7, no. 4, pp. 374–386, 2014.

[6] S. Athani, P. Kharel, D. Airey, and P. Rognon, "Grain-size effect on uplift capacity of plate anchors in coarse granular soils," *Géotechnique Letters*, vol. 7, no. 2, pp. 167–173, 2017.

[7] T. M. Evans and N. Zhang, "Three-dimensional simulations of plate anchor pullout in granular materials," *International Journal of Geomechanics*, vol. 19, no. 4, Article ID 04019004, 2019.

[8] B. M. Das, "Model tests for uplift capacity of foundations in clay," *Soils and Foundations*, vol. 18, no. 2, pp. 17–24, 1978.

[9] S. P. Singh and S. V. Ramaswamy, "Influence of frequency on the behaviour of plate anchors subjected to cyclic loading," *Marine Georesources & Geotechnology*, vol. 26, no. 1, pp. 36–50, 2008.

[10] S. P. Singh and S. V. Ramaswamy, "Effect of shape on holding capacity of plate anchors buried in soft soil," *Geomechanics and Geoengineering*, vol. 3, no. 2, pp. 157–166, 2008.

[11] J. Liu, M. Liu, and Z. Zhu, "Sand deformation around an uplift plate anchor," *Journal of Geotechnical and Geoenvironmental Engineering*, vol. 138, no. 6, pp. 728–737, 2012.

[12] S. H. Chow, C. D. O'Loughlin, C. Gaudin, and J. T. Lieng, "Drained monotonic and cyclic capacity of a dynamically installed plate anchor in sand," *Ocean Engineering*, vol. 148, pp. 588–601, 2018.

[13] S. K. Dash and A. K. Choudhary, "Geocell reinforcement for performance improvement of vertical plate anchors in sand," *Geotextiles and Geomembranes*, vol. 46, no. 2, pp. 214–225, 2018.

[14] C. Gaudin, C. D. O'Loughlin, M. F. Randolph, and A. C. Lowmass, "Influence of the installation process on the performance of suction embedded plate anchors," *Géotechnique*, vol. 56, no. 6, pp. 381–391, 2006.

[15] C. Gaudin, H. T. Kien, and S. Ouahsine, "Plate anchor failure mechanism during keying process," in *Proceedings of the Eighteenth International Offshore and Polar Engineering Conference*, Vancouver, Canada, July 2008.

[16] M. Randolph, C. O'Loughlin, C. Gaudin, and A. Lowmass, "Physical modelling to assess keying characteristics of plate anchors," *Physical Modelling in Geotechnics*, vol. 1, pp. 659–665, 2006.

[17] Z. Song, Y. Hu, C. O'Loughlin, and M. F. Randolph, "Loss in anchor embedment during plate anchor keying in clay," *Journal of Geotechnical and Geoenvironmental Engineering*, vol. 135, no. 10, pp. 1475–1485, 2009.

[18] A. Blake, "Centrifuge modelling to assess consolidation following keying of directly embedded plate anchors," in *Proceedings of the 21st European Young Geotechnical Engineers Conference (EYGEC 2011)*, Rotterdam, The Netherlands, September 2011.

[19] M. Yang, C. P. Aubeny, and J. D. Murff, "Behavior of suction embedded plate anchors during keying process," *Journal of Geotechnical and Geoenvironmental Engineering*, vol. 138, no. 2, pp. 174–183, 2012.

[20] L. H. Lu, "Rotational adjustment process of plate-shaped gravity installation anchor and suction-type installation plate anchor in clay," Master thesis, Dalian University of Technology, Dalian, China, 2015.

[21] R. S. Merifield, S. W. Sloan, and H. S. Yu, "Stability of plate anchors in undrained clay," *Géotechnique*, vol. 51, no. 2, pp. 141–153, 2001.

[22] R. S. Merifield, A. V. Lyamin, S. W. Sloan, and H. S. Yu, "Three-dimensional lower bound solutions for stability of plate anchors in clay," *Journal of Geotechnical and Geoenvironmental Engineering*, vol. 129, no. 3, pp. 243–253, 2003.

[23] B. M. Das, "Uplift capacity of plate anchors in clay," in *Proceedings of the 4th International Offshore and Polar Engineering Conference*, vol. 1, pp. 436–442, Osaka, Japan, 1994.

[24] B. M. Das, E. C. Shin, R. N. Dass, and M. T. Omar, "Suction force below plate anchors in soft clay," *Marine Georesource and Geotechnology*, vol. 12, no. 1, pp. 71–81, 1994.

[25] D. P. Stewart and M. F. Randolph, "T-bar penetration testing in soft clay," *Journal of Geotechnical Engineering*, vol. 120, no. 12, pp. 2230–2235, 1994.

[26] X. Ou, X. Zhang, J. Fu, C. Zhang, X. Zhou, and H. Feng, "Cause investigation of large deformation of a deep excavation support system subjected to unsymmetrical surface loading," *Engineering Failure Analysis*, vol. 107, p. 105202, 2020.

[27] J. Zhang, T. Feng, F. Zhang, and W. Li, "Experimental study on improvement of seawall filler materials composed of sea sand and sea mud," *Marine Georesources & Geotechnology*, vol. 38, no. 2, pp. 193–203, 2020.

[28] M. Zhou, M. S. Hossain, Y. Hu, and H. Liu, "Behaviour of ball penetrometer in uniform single- and double-layer clays," *Géotechnique*, vol. 63, no. 8, pp. 682–694, 2013.

[29] M. Zhou, M. S. Hossain, Y. Hu, and H. Liu, "Scale issues and interpretation of ball penetration in stratified deposits in centrifuge testing," *Journal of Geotechnical & Geoenvironmental Engineering*, vol. 142, no. 5, Article ID 04015103, 2016.

[30] H. Ma, M. Zhou, Y. Hu, and M. S. Hossain, "Interpretation of layer boundaries and shear strengths for soft-stiff-soft clays using CPT data: LDFE analyses," *Journal of Geotechnical & Geoenvironmental Engineering*, vol. 142, no. 1, Article ID 04015055, 2016.